Effect of hydrogen and oxygen on stability of expanders and performance of lead/acid batteries

D. Pavlov, S. Gancheva and P. Andreev

Central Laboratory of Electrochemical Power Sources, Bulgarian Academy of Sciences, Sofia 1113 (Bulgaria)

Abstract

Expanders are organic additives to the negative active mass that increase plate capacity, especially at low temperatures. They operate under constant hydrogen and oxygen attack at strongly negative potentials as a result of which they undergo degradation. This leads to changes in plate capacity, which may limit the life of the battery. The aims of the present work are: (i) to suggest a method for determining the effect of hydrogen, oxygen and the potential on the stability of expanders; (ii) to identify some of the structural groups in organic compounds that exert an efficient expander action. The influence of Velex, Mimosa, Quebraco, Syntan NK (SNK) and EZE–Skitan on the electrochemical characteristics and the life of negative battery plates has been investigated. It is established that structural groups of the pyrocatechin type (Quebraco and EZE–Skitan) have effective expander action. Quebraco increases the plate capacity during the first cycles. EZE–Skitan increases the capacity of the plates after 50 to 60 charge/discharge cycles, when disintegration of its structure, probably to pyrocatechin groups, proceeds. By applying a new method for determining the expander stability, it is found that expanders containing pyrocatechin structural groups are more easily oxidized than hydrogenated. It is concluded that the most effective expander should be a combination of several compounds with different stabilities to oxidation and reduction. Appropriate expanders should be selected for each type of battery.

Introduction

Expanders (EXR) are organic agents added to the lead active mass (LAM) to ensure high capacity of the battery during its service life. There are two basic problems related to the selection of expanders: (i) they should facilitate the formation of a LAM structure that gives high battery capacity, especially at low temperatures; (ii) they should be chemically resistant to the strongly aggressive medium in which the negative battery plate operates. On battery charge, hydrogen is evolved at the negative plate which may cause reduction of the expander. The latter is also subjected to oxidation by the oxygen that diffuses from the positive plate. The lead battery plate operates under strongly negative potentials that may induce changes in the distribution of electrons in the expander molecules and hence affect their stability.

With the valve-regulated design of lead/acid battery, the flow of oxygen evolved at the positive plate is forced towards the negative plate. This makes the expander stability to oxidation even more important. Very often, efficient expanders in traditional batteries undergo rapid chemical degradation and the plates lose capacity. Hence, it is important to determine the expander resistance to both reduction and oxidation.

The stability of the expander is determined by its structure. There is a relation between the expander structure and the energy characteristics of the electrodes. Numerous attempts have been made to disclose the most sophisticated relation [1–6]. Nevertheless, there are no data available in the literature on the processes of expander degradation under the action of oxygen or hydrogen. Elucidation of these processes has become increasingly important with the introduction of valve-regulated batteries. The aim of the work reported here is, first, to suggest a possible method for obtaining information about the stability of expanders on oxidation and reduction and, second, to identify some structural groups in organic substances that act like expanders.

Experimental

Preparation of negative plates and cells

Commercial automotive grids cast from a Pb–6wt.%Sb alloy were used to prepare the plates. The paste was produced from leady oxide (70% degree of oxidation), 0.2 wt.% carbon black, 0.4 wt.% $BaSO_4$, 0.3 wt.% EXR (or without expander) mixed with H_2O and H_2SO_4 solution (sp. gr. 1.40) in a H_2SO_4/PbO ratio of 4.5%. The density of the paste was 4.2 g cm^{-3}. The rated capacity of the negative plates was 11 Ah at an active mass utilization of 42%. The test cells contained one negative plate, two positive plates and H_2SO_4 of sp. gr. 1.28.

Investigation of negative plates

The following parameters were investigated:
(i) initial performance of negative plates:
- cold-cranking ability ($I = 3.5$ C/4 A, $t = -18$ °C)
- capacity at 4-h rate of discharge ($I = 0.25$ C/4 A, $t = 25$ °C)
- potential/time transients during charge ($I = 0.2$ C/4 A, $t = 25$ °C)

(ii) plate cycle life on deep discharge cycling;
(iii) structure and crystal morphology of LAM studied by scanning electron microscopy (SEM) observations of the active mass in the charged and discharged state, and examination of its skeleton;
(iv) determination of the chemical stability of the expander under oxygen and hydrogen attack.

Determination of the effect of hydrogen and oxygen on expander stability

After determining the capacity (C/4), the plate under investigation was charged and placed in a cell containing two Pb/PbO$_2$ elements under overcharge ($I_{ch} = 2$ A/ element) and an H_2SO_4 of sp. gr. 1.28 (Fig. 1). A constant cell temperature of 50 °C was maintained. To avoid mechanical contact between the plates of the Pb/PbO$_2$ elements and the test plate, a set of spacing ribs was used. To study the effect of hydrogen on the stability of the expanders, the test plate was placed between negative plates under overcharge. The negative plates of the two elements created a hydrogen atmosphere around the investigated electrode and this caused hydrogenation of the expander. The rate of the reaction of hydrogenation was determined using the following method. At given intervals, the investigated plate was removed from the hydrogen atmosphere and inserted into the test cell. After charge, the capacity (C/4) was measured. Then, the plate was charged again and returned to the hydrogen atmosphere in the hydrogenation cell.

The effect of oxygen on the expanders was determined by using similar cells. In this case, however, the test plate was placed between the positive plates of the two
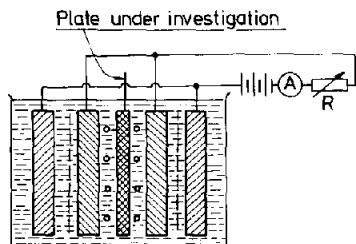
Fig. 1. Schematic of experimental cell.

elements under overcharge (Fig. 1). Thus, the test plate was surrounded by an oxygen atmosphere.

Expanders and their structure

Expanders with different structural units and different efficiency on the capacity of negative plates were chosen, i.e., natural products (Velex, Quebraco and Mimosa); synthetic products (EZE–Skitan and Syntan NK). The basic structural units of these expanders are presented in Fig. 2.

Velex is a lactone of ellagic acid (Fig. 2(a)), bonded to glucose by ester or glycosidic bonds [7]. It undergoes hydrolysis in dilute acidic solutions whereby the ester and glycosidic bonds are broken and the molecule disintegrates into compounds with a simpler structure. Quebraco and Mimosa are condensed catechols. Quebraco-catechol is of the pyrocatechin type (Fig. 2(b)) and Mimosa catechol of the pyrogallol type (Fig. 2(c)). EZE–Skitan is obtained as a result of condensation of lignosulfonic acids and phenols by formaldehyde. The basic structural units of lignin are phenylpropane structural group derivatives of pyrocatechin (Fig. 2(d_1)) [8]. In the process of sulfite extraction of cellulose, sulfonation of the propane chains in the lignin molecule leads to the formation of lignosulfonic acids (Fig. 2(d_2)). Condensation of lignosulfonic acids with phenols through formaldehyde results in the formation of spacial network structures in which pyrocatechin groups are involved spacially and, thus, decrease their activity. With degradation of these structures, the activity of pyrocatechin increases. Syntan NK consists of naphthalenesulfonic acids condensed through formaldehyde and then neutralized [7].

Results

Discharge characteristics

The initial performance parameters of negative plates were determined first. Figure 3(a) presents the discharge transients with a current $I = 0.25$ $C/4$ A at 25 °C, while Fig. 3(b) shows those obtained during cold cranking tests of the cells.

Expanders (except Mimosa) increase the polarization of the plates. In both types of discharge, expanders increase the time of discharge. This effect is more pronounced at low temperatures. Consequently, all changes in capacity of the negative plate above the values measured for plates without expander ($\Delta t_{exp.c.}$, $\Delta t_{exp.c.a.}$) will be determined by the changes in structure and properties of the expander. These changes lead to changes in the structure of LAM and, hence, in battery capacity. The longest time of discharge is exhibited by plates containing Syntan NK (SNK), followed by Quebraco, EZE–Skitan, and Velex with the weakest effect.
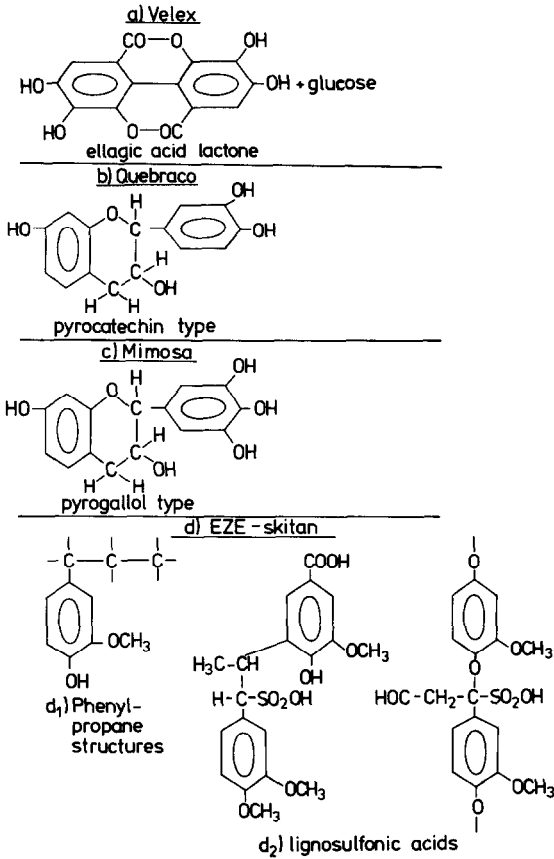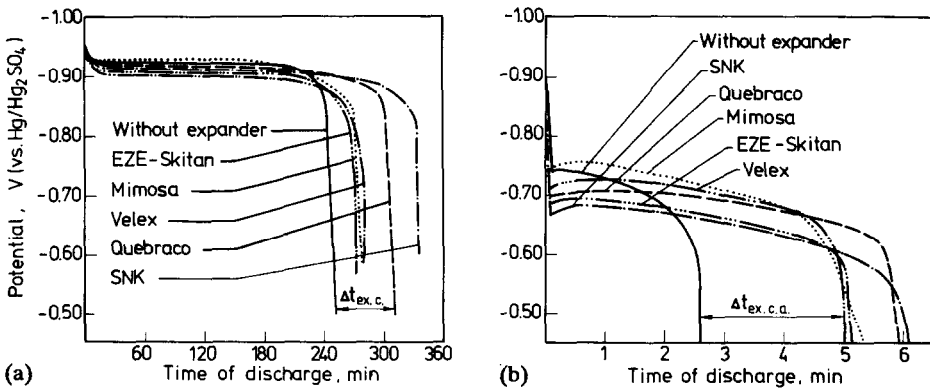
a) Velex

HO, HO — ellagic acid lactone + glucose

ellagic acid lactone

b) Quebraco

HO — OH OH

pyrocatechin type

c) Mimosa

HO — OH OH OH

pyrogallol type

d) EZE - skitan

d_1) Phenyl-propane structures

OCH$_3$
OH

COOH
OCH$_3$
OH

H$_3$C-CH
H-C-SO$_2$OH
OCH$_3$
OCH$_3$

OCH$_3$
HOC-CH$_2$-C-SO$_2$OH
OCH$_3$
O

d_2) lignosulfonic acids

Fig. 2. Structural units of expanders.

Fig. 3. Discharging transients of negative plates with/without expander: (a) capacity; (b) cold-cranking tests.

Charge characteristics

Figure 4 shows the changes in plate potential on charging with $I = 0.2$ $C/4$ A at 25 °C. Expanders increase both the charging potential of the plates (line A) and the hydrogen overvoltage (line B). Both reactions are inhibited by expanders.

Cycling

Figure 5 presents the changes in capacity during cycling with 60% depth-of-discharge. Expanders prolong the life of the cells. Three profiles of the capacity curves are observed:

(i) The capacity of the plates with the Velex and Mimosa exhibits a gradual decline which indicates that the expanders undergo unfavourable degradation.
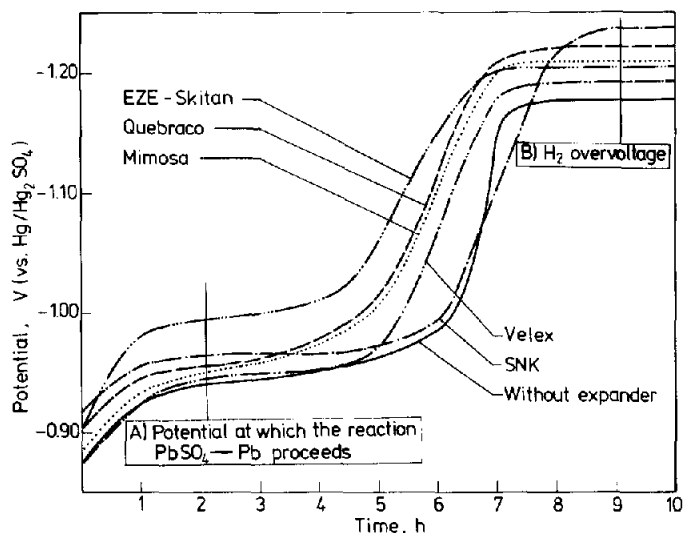

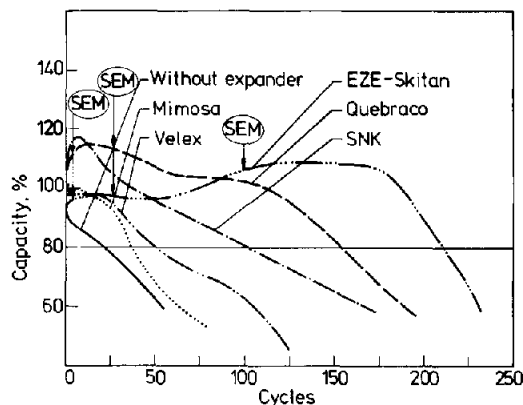Fig. 4. Charging transients of negative plates with/without expander.

Fig. 5. Changes in capacity during cycling of cells with negative plates with/without expander. Cycles during which samples were taken from the plates for SEM observations are marked with 'SEM'.

(ii) The capacity of plates with Syntan NK (SNK) and Quebraco displays a rapid initial increase that passes through a maximum and declines thereafter. This indicates that, in their natural forms, these compounds are less active. During the first five cycles, they undergo changes that convert them into more active forms and thus increase the capacity of the negative plates. After a certain number of cycles, a process of unfavourable expander degradation starts and the plate capacity declines.

(iii) EZE–Skitan is not very active at the beginning of cycling, but it is sufficiently stable to maintain a constant plate capacity for almost 50 cycles. After that, degradation of the expander to more active forms starts and the plate capacity increases until the 175th cycle when the capacity begins to decline. All this ensures a long battery life.

Scanning electron microscope observations

Figure 6(a) presents a micrograph of the charged active mass of plates with Quebraco (3rd cycle). The active mass is composed of small lead crystals. Fig. 6(b) shows a micrograph of the same plate after a 4-h discharge (3rd cycle). Well-shaped $PbSO_4$ crystals are observed. When they are dissolved in CH_3COONH_4 solution, the lead skeleton of the active mass can be seen (Fig. 6(c)). The active-mass skeleton is built of interconnected dendrites. The lead crystals taking part in the current-generation process are situated over this skeleton (energetic structure). The skeleton conducts the electric current from every point of the lead active mass to the plate grid. Its stability determines the life of the battery [9, 10].

Figure 7 shows the skeleton structure and the morphology of the dendrites of plates with Quebraco at the 3rd and 25th cycles. At the 3rd cycle, the skeleton is covered by needle-like crystals over which 'energetic' lead crystals are situated (Fig. 7(a). The capacity is relatively low and is below the maximum of the capacity/cycle number-curve (Fig. 5). After 25 cycles (Fig. 7(b)), the skeleton structure features larger pores and the needle-like crystals over the skeleton have disappeared. The skeleton is covered by small grain-like crystals. Obviously, the expander that controls the phase generation and the growth of the lead crystals has undergone some changes. Probably, these changes are also responsible for the maximum observed in the capacity/cycle-number curve in Fig. 5.

Figure 8 presents the structure and morphology of the dendrites that build the LAM skeleton of plates with EZE–Skitan at the 3rd, 25th and 100th cycles. The following skeleton evolution is observed. At the 3rd cycle, the skeleton is built of small dendrites. After 25 cycles the small dendrites are grouped together into large agglomerates, and after 100 cycles the skeleton features a much smoother surface, thinner dendrites and higher microporosity. The highest plate capacity is measured at the 100th cycle (Fig. 5).

During cycling, part of the skeleton (10–20%) participates in the current-generation process. This part is subjected to the action of the expander in the form corresponding to the respective cycle. Under the action of hydrogen, oxygen and the potential, the expander undergoes continuous degradation and/or condensation of some of its components after that. Thus, formation of lead crystals during the different cycles proceeds under the action of different expander components. That is why the lead crystals and the active mass skeleton undergo evolution in structure and morphology during cycling.

During evolution of the LAM structures, some of the dendrites may become so thin that, when the $PbSO_4$ crystals are dissolved in the CH_3COONH_4 solution, the skeleton may disintegrate into powder. This is associated with increased polarization, that excludes some regions of the LAM from the process of current generation, and battery failure. This evolution is controlled by the action of the expander and of its
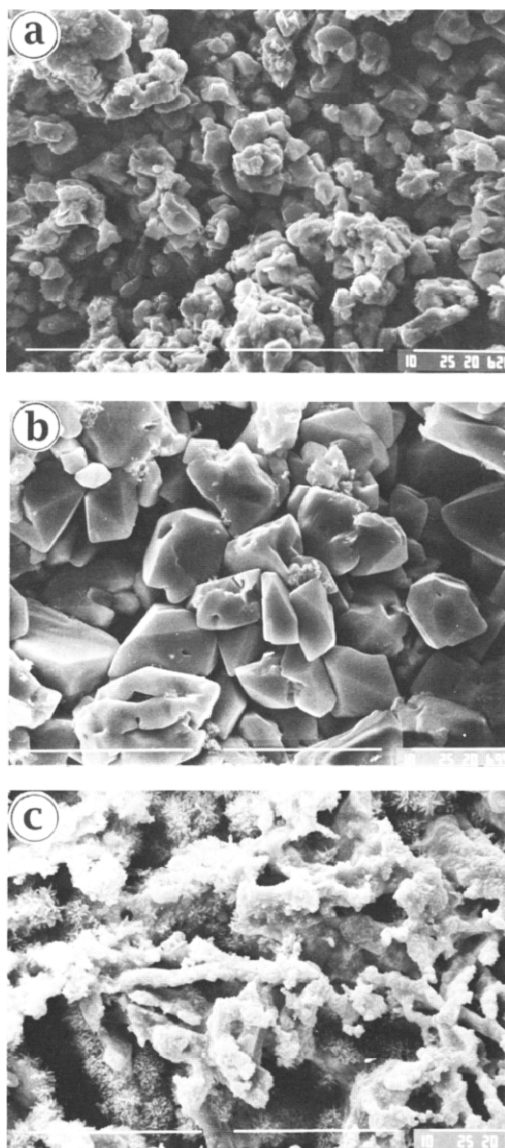
Fig. 6. Micrographs of LAM with Quebraco at 3rd cycle: (a) charged active mass; (b) discharged active mass; (c) skeleton structure of active mass. White line corresponds to 10 μm.

products obtained on battery operation. Hence, it is of crucial importance to establish the effect of hydrogen, oxygen and the potential on the processes of expander degradation, in order to find the most stable and most effective expander for each type of lead/acid battery.

Expander stability

Investigations were performed using plates with expanders that ensured long battery life, i.e., Quebraco and EZE–Skitan. The resulting capacity curves as a function
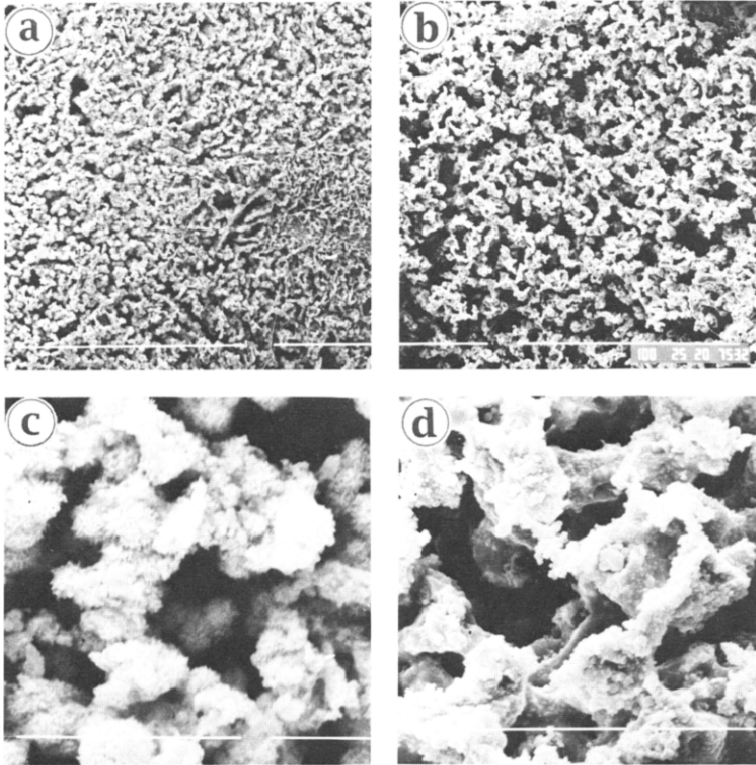
Fig. 7. Skeleton structure (upper micrographs) and crystal morphology (lower micrographs) of active mass with Quebraco after 3 cycles (a, c); 25 cycles (b, d). White line corresponds to 100 μm (upper photos) and 10 μm (lower photos).

of the time of oxidation and reduction are presented in Fig. 9. The plate capacity during the first cycle was taken as the 100% value. All of the other capacities were calculated with reference to that value. Besides the plates subjected to oxidation and reduction, reference negative plates with the same expanders were left in the test cells with no hydrogen and oxygen attack.

Figure 5 shows that the capacity of the plates containing EZE–Skitan remains almost constant for about 50 cycles and starts increasing after that. The data in Fig. 9 indicate that the capacity of the reference plate with EZE–Skitan also preserves an almost constant value. When the plate is subjected to oxygen attack, however, its capacity increases by about 10% and changes but slightly during 20 days of oxygen aggression. Under the action of hydrogen, the expander EZE–Skitan is modified in such a way that its products increase the capacity of the plate by about 15%. This value is relatively stable during the next 20 days of hydrogen influence. This means that the products obtained under the action of oxygen and hydrogen are more-effective expanders and are sufficiently stable on oxidation and hydrogenation. Figure 5 shows that these expander products are formed after 50 charge/discharge cycles as a result of which the capacity of the plates with EZE–Skitan is increased. After about 175 cycles (Fig. 5), degradation of the expander starts and it is converted into a nonactive form, which leads to a decline in plate capacity and battery failure.
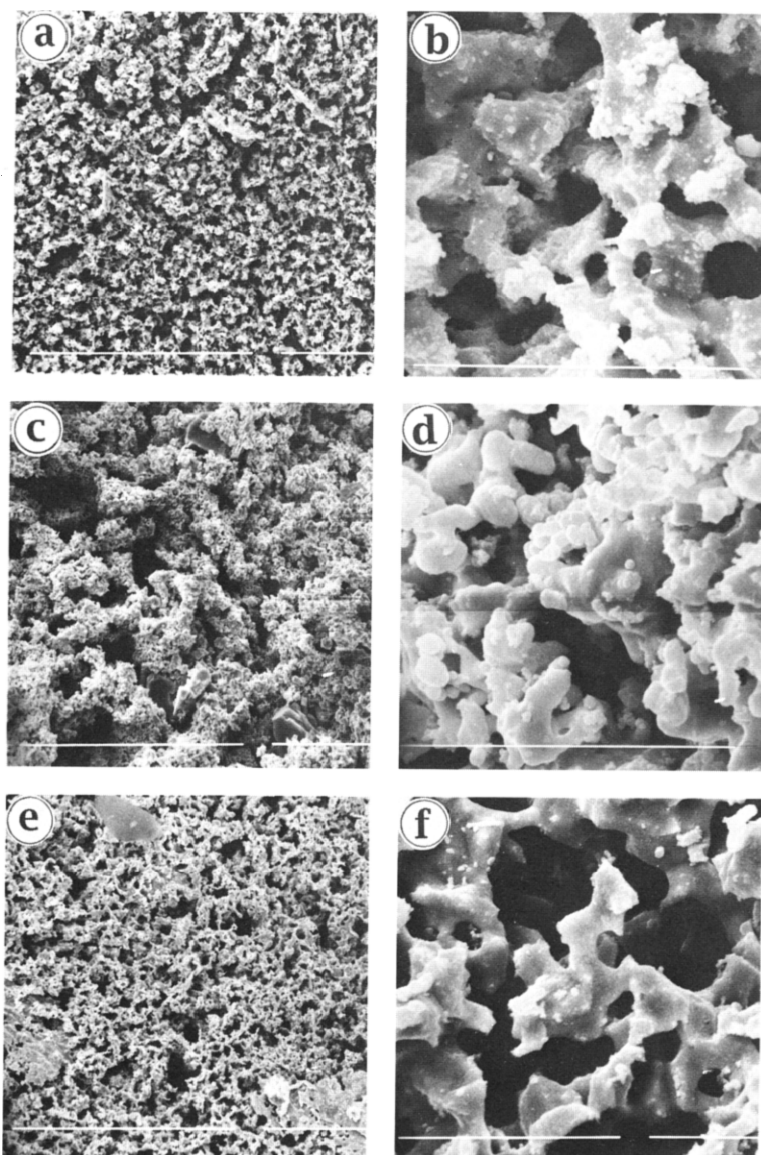
Fig. 8. Skeleton structure (left-hand micrographs) and crystal morphology (right-hand micrographs) of the active mass with EZE–Skitan after 3 cycles (a, b); 25 cycles (c, d); 100 cycles (e, f). White line corresponds to 100 μm (a, c and e) and 10 μm (b, d and f).

The data in Fig. 5 indicate that the capacity of negative plates with Quebraco increases during the first 10 to 12 cycles and, after a maximum, starts to decrease continuously at a variable rate. Figure 9(b) shows that when there is no hydrogen or oxygen action, the capacity of negative plates grows for a period of 20 days. Probably, the Quebraco product is a more effective expander than the initial compound. When the plates are subjected to hydrogen attack, their capacity increases slightly and starts
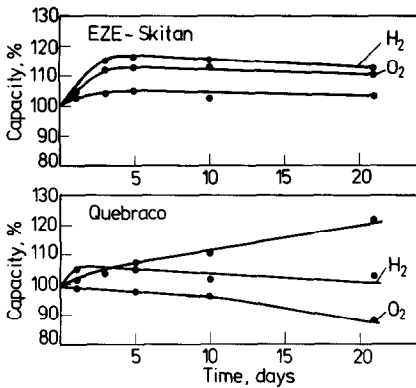
Fig. 9. Capacity curves as a function of time of oxygen and hydrogen attack for plates with Quebraco or EZE–Skitan, and for reference plates not subjected to such action.

to decline gradually thereafter. The effect of oxygen on the degradation of the expander is even more pronounced, especially after 10 days of exposure. The oxidation products of Quebraco are ineffective as expanders.

The results from the capacity measurements performed with plates subjected to oxygen, hydrogen and potential impact are in good agreement with the curves obtained from the battery-life tests (Fig. 5). This may be a confirmation of the hypothesis that changes in plate capacity on cycling are due largely to the changes in structure and properties of the expanders contained.

Discussion

On comparing the results presented in Figs. 3, 5 and 9, it can be seen that expanders containing structural groups of the pyrocatechin type have the most beneficial effect on the electrical parameters and the life of negative battery plates. Such expanders are Quebraco and EZE–Skitan. Pyrocatechin groups in Quebraco exert an immediate effect on cycling. They ensure high battery capacity and long cycle life (Fig. 5). Pyrocatechin groups in EZE–Skitan are connected in more complex spacial structures and, hence, the initial plate capacity is considerably lower than that of plates containing Quebraco. Only after 50 to 60 cycles, when disintegration of the molecules of EZE–Skitan occurs, the effect of pyrocatechin structural groups is displayed more clearly.

Figure 9 shows that plates with Quebraco lose capacity faster when exposed to oxygen than when hydrogenated. This may be due to an easier degradation of pyrocatechin structural groups under the action of oxygen. The degradation may reach as far as breaking of the benzene nuclei. This process is markedly slowed down in EZE–Skitan.

Figure 5 indicates that Mimosa has the effect of an expander, but is rather unstable and hence the plate life is too short. It is known that structural groups of the pyrogallol type are readily attacked, especially electrochemically. Barnes [6] has established also that Quebraco is an effective expander, while Mimosa is not.

The results in Fig. 9 show that the proposed method for determining the stability of expanders towards hydrogen and oxygen attack may be applied successfully to select appropriate expanders for the negative plates of various types of lead/acid batteries (valve-regulated, stationary, automotive, etc.).

It can be concluded from the results presented in Fig. 5 that the effective expander with lasting action should be a combination of several compounds with different stabilities to the influence of oxygen, hydrogen and potential, and containing active structural groups (of the pyrocatechin type for example) both at the beginning of battery operation and during the whole service life of the battery.

References

1 E.J. Ritchie, *Trans. Electrochem. Soc.*, 92 (1947) 229–257.
2 E.J. Ritchie, *J. Electrochem. Soc.*, 100 (1953) 53–59.
3 H. Niklas and H. Jakobljevich, *J. Appl. Electrochem.*, 2 (1972) 165–167.
4 W. Simon, *Bosch Tech. Ber.*, 1 (1966) 234–251.
5 E.G. Yampol'skaya, I.A. Smirnova, M.I. Yershova, S.A. Sapotnitskiy and L.I. Kryukova, *Electrokhimiya*, 8 (1972) 1325–1328.
6 S.C. Barnes, in *Lead 65, Proc. 2nd Int. Conf. on Lead, Arnhem, Netherlands, 1965,* Pergamon, Oxford, 1967, pp. 219–226.
7 M. Pesheva, *Chemistry and Physics of Raw Leather and of Tanning Agents,* (Bulgarian), Publisher Ministry of Education — Higher Institute of Chemical Technology, Sofia, Bulgaria, 1982, Ch. 5, pp. 204–273.
8 K.V. Sarkanen and C.H. Ludwig, in K.V. Sarkanen and C.H. Ludwig (eds.), *Lignins,* Lesnaya Promishlenost, Moscow, 1975, Ch. 1, pp. 9–18 (Russian translation).
9 D. Pavlov and V. Iliev, *J. Power Sources,* 7 (1981/82) 153–164.
10 V. Iliev and D. Pavlov, *J. Appl. Electrochem.,* 15 (1985) 39–52.